



# Elevation Accuracy Assessment of Aerial LiDAR against Total Station for Topographic Mapping under Diverse Terrain Conditions

Iqbal Hanun Azizi, Purnama Budi Santosa, Fadila Sobasita, Nurrohmat Widjajanti

Department of Geodesy Engineering, Faculty of Engineering UGM, Yogyakarta, Indonesia

**Correspondent Author :** Iqbal Hanun Azizi | **Email:** [i.hanun.azizi@ugm.ac.id](mailto:i.hanun.azizi@ugm.ac.id)

Diterima (*Received*): 30/Sep/2025 Direvisi (*Revised*): 30/Oct/2025 Diterima untuk Publikasi (*Accepted*): 03/Nov/2025

## ABSTRACT

Topographic mapping requires precise three-dimensional (3D) coordinates for geospatial applications. Conventional terrestrial surveys using Total Station (TS) and GNSS-RTK provide reliable accuracy but are time-consuming. Aerial LiDAR offers a faster alternative by generating high-density point clouds with wide coverage, although its accuracy must be evaluated. This study assesses the elevation accuracy of LiDAR compared to TS across six terrain categories: open ground surface, vegetation-covered surface, road section, sparsely populated settlement, densely populated settlement, and river. Data acquisition employed a 1 m grid to align horizontal coordinates and focused on elevation values. The evaluation included descriptive statistics, elevation difference histograms, Root Mean Square Error (RMSE), and linear correlation analysis. Results indicate that LiDAR achieved high accuracy in open ground and road sections, with low RMSE and correlation values equal to one. Accuracy decreased in settlements due to roof and wall reflections, and in dense vegetation where laser pulses were blocked by canopy. Despite these limitations, LiDAR effectively represented contour patterns after filtering, classification, and breakline addition. In rivers, LiDAR produced the largest deviations caused by water reflectivity, while TS remained precise for riverbed elevations. This study demonstrates that LiDAR is highly effective for mapping open areas and roads, applicable in settlements with further processing, and still useful in vegetated terrain through its multiple-return capability. However, water bodies require TS validation as a precision reference. Overall, LiDAR provides efficient wide-area data acquisition, while TS continues to serve as the precision standard in complex conditions under ISO/IEC 17025. The application of ISO/IEC 17025 is essential to ensure that measurement, calibration, and data validation comply with principles of accuracy, traceability, and uncertainty control, thereby making topographic mapping results accountable.

**Keywords:** LiDAR, Total Station, Coordinate, Accuration, ISO/IEC 17025.

© Author(s) 2025. This is an open access article under the Creative Commons Attribution-ShareAlike 4.0 International License (CC BY-SA 4.0).

## 1. Introduction

Topographic mapping provides geospatial information for spatial planning, natural resource management, disaster mitigation, and infrastructure development. It produces a three-dimensional (3D) model of the Earth's surface, known as a Digital Elevation Model (DEM) (Guth et al., 2021). A DEM consists of 3D coordinates (X, Y, Z) that form a surface representation of the Earth. The accuracy of DEM elevation plays a critical role in the quality of geospatial analysis; therefore, every mapping method must generate precise and accountable data (Saleem et al., 2019). Although 3D coordinate acquisition technologies have advanced, their results have not been directly validated against the Total Station (TS), an instrument that directly measures objects with high precision. TS integrates an electronic theodolite, Electronic Distance Meter (EDM), and electronic data recorder into a single measurement system that produces coordinate data (Basuki, 2011). TS remains a

highly precise mapping technology because the measured object is observed directly. Meanwhile, modern mapping technologies such as Unmanned Aerial Vehicle (UAV) LiDAR have rapidly developed due to their ability to generate point cloud coordinates efficiently, particularly in areas that are difficult to access (Ding & Chen, 2024). UAV LiDAR employs multi-echo technology that enables laser pulses to penetrate vegetation layers, reaching the ground through canopy gaps (Chen et al., 2015). Although UAV LiDAR offers rapid data acquisition, its point cloud coordinates must be validated against TS measurements to ensure accuracy and traceability.

Engineering Survey Laboratories are required to verify that UAV LiDAR measurements comply with international quality standards. The International Organization for Standardization (ISO) and the International Electrotechnical Commission (IEC) 17025:2017, abbreviated as ISO/IEC 17025, mandate that measurement,

instrument calibration, and data validation adhere to principles of accuracy, traceability, and uncertainty control (Khodabocus, 2011). Laboratories implement this standard to guarantee that topographic data quality is accountable. This study evaluates UAV LiDAR elevation data by comparing it with TS measurements as a reference under ISO/IEC 17025 principles. The evaluation focuses on the precision and accuracy of UAV LiDAR-derived elevations across varying surface conditions. The study also tests elevation values across different land cover categories, including open ground surface, vegetation-covered surface, road section, sparsely populated settlement, densely populated settlement, and river.

## 2. Data and Methodology

This study utilized coordinate data acquired from UAV LiDAR and TS measurements as precision references. LiDAR acquisition produced point clouds, while TS collected detailed topographic points using detail and spot height methods. Data were collected across six terrain categories: open ground surface, vegetation-covered surface, road section, sparsely populated settlement, densely populated settlement, and river. LiDAR data were

processed through slope-based point cloud classification and the addition of breaklines to preserve geomorphological authenticity. TS data acquisition applied trigonometric principles to derive planimetric coordinates (X, Y) and elevation (Z). To align the datasets, both LiDAR and TS coordinates were resampled to a 1 m grid, ensuring horizontal consistency (X, Y) and focusing the comparison on elevation (Z). The evaluation included the assessment of minimum and maximum elevation values, histogram analysis of elevation differences, Root Mean Square Error (RMSE) calculation, and linear correlation analysis to determine LiDAR accuracy relative to TS.

### 2.1. Study Area and Data

LiDAR and TS data acquisition was conducted in a study area characterized by diverse terrain conditions (Figure 1). The study area covered six categories: open ground surface, vegetation-covered surface, densely populated settlement, sparsely populated settlement, road section, and river. This categorization aimed to compare LiDAR-derived elevations with TS measurements under varying terrain conditions. Accordingly, the analysis assessed how vegetation obstructions, building density, and corridor features such as rivers and roads influenced the elevation accuracy of both methods.

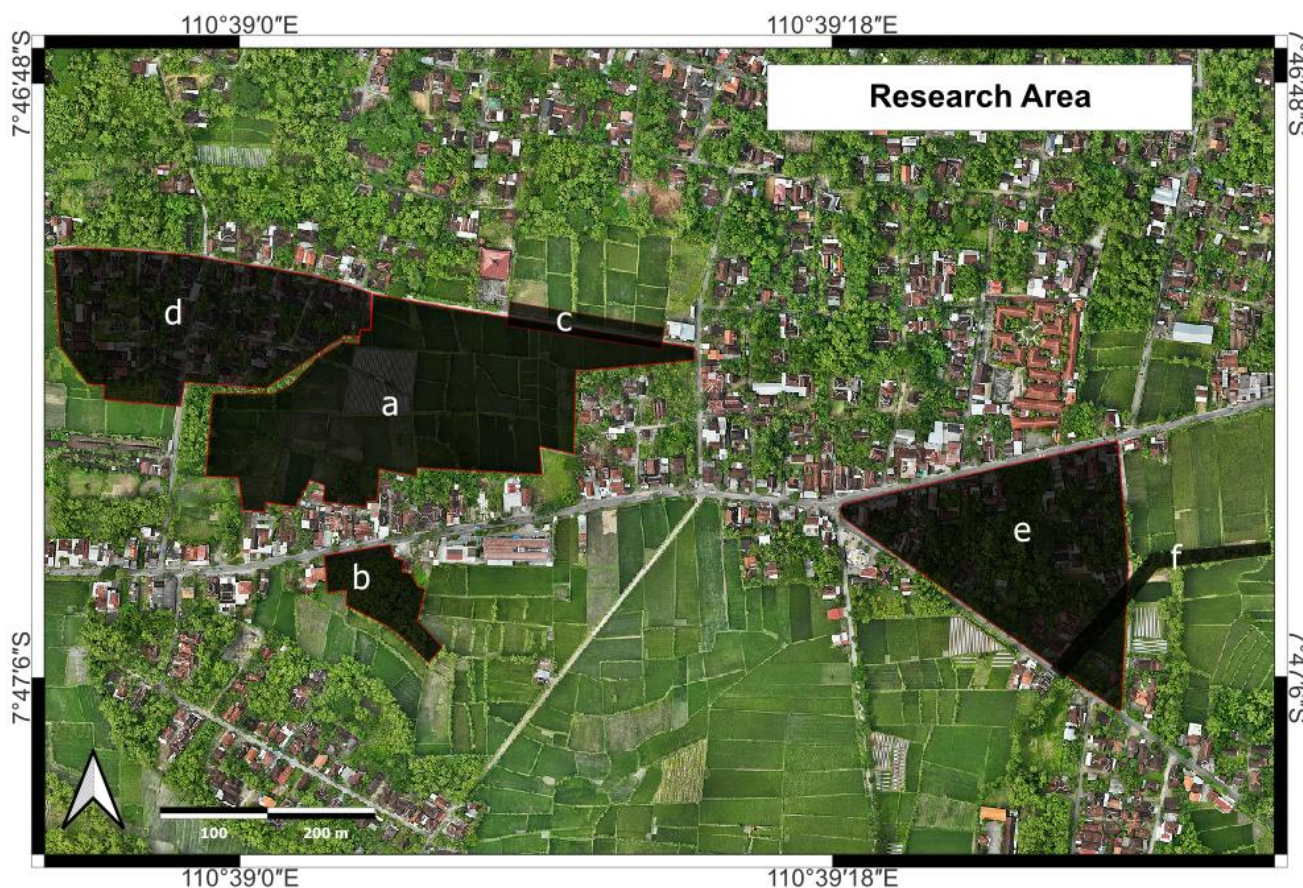


Figure 1 Study area categories for UAV LiDAR and TS: (a) open ground surface, (b) vegetation-covered surface, (c) road section, (d) sparsely populated settlement, (e) densely populated settlement, and (f) river

LiDAR data were collected using a UAV quadcopter generating based on point clouds. TS measurements applied detail and spot height methods to capture both natural and man-made topographic features, including buildings, road edges, embankments, channels, trees, fences, and others. The measured points selectively represented topographic variations with varying point densities. LiDAR data acquisition was conducted over three days, while TS measurements were completed over ten days. Both LiDAR and TS data were collected under similar times, temperatures, and weather conditions to ensure consistency.

## 2.2. Total Station Data Acquisition

TS coordinate acquisition is a process of directly obtaining detailed topographic positions in the field. The collected coordinates are then processed into maps that accurately represent the Earth's surface (Basuki, 2011). Detailed coordinates include both natural and man-made features in planimetric and elevation aspects, using a polar method approach. This method determines a point's position through angle and distance measurements. The calculation principles for planimetric (Figure 2) and vertical coordinates in TS are based on triangular trigonometry (Figure 3), as expressed in Equations (1) to (5) (Basuki, 2011; Olawuyi & Okeniyi, 2023).

$$X_t = X_{STN} + d \cdot \sin \alpha \quad (1)$$

$$Y_t = Y_{STN} + d \cdot \cos \alpha \quad (2)$$

$$v = d \cdot \tan h \quad (3)$$

$$\Delta h = t_{STN} + vd - t_{refl} \quad (4)$$

$$H_t = H_{STN} + \Delta h \quad (5)$$

where:

- $X_t, Y_t$  : coordinates of the target detail point
- $X_{STN}, Y_{STN}$  : coordinates of the instrument station
- $d$  : horizontal distance
- $\alpha$  : azimuth angle
- $h$  : helling
- $vd$  : vertical distance
- $\Delta h$  : elevation difference
- $t_{STN}$  : instrument height
- $t_{ref}$  : reflector height
- $H_{STN}$  : known elevation of the instrument station
- $H_t$  : elevation (Z) of the target detail point

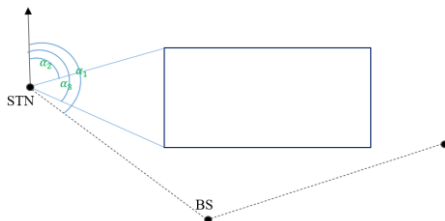


Figure 2 Detailed measurement of the planimetric situation using the polar method

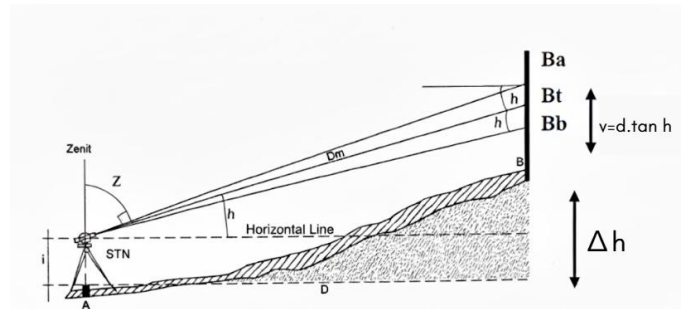


Figure 3 Detailed measurement of elevation using the trigonometry method

## 2.3. LiDAR Data Acquisition

LiDAR is a remote sensing technology that utilizes laser beams to measure distances between the sensor and objects on the Earth's surface. The LiDAR system emits laser pulses toward a target and detects the reflected pulses, enabling distance measurement based on the time it takes for the light to return (Killinger, 2014). LiDAR sensors operate on the principle of active scanning, allowing the transmitter unit to generate thousands to millions of laser pulses per second. These laser pulses strike various objects such as the ground, vegetation, or buildings, and the receiver sensor detects the reflection of each returning pulse. The system can adjust the laser direction in real-time, allowing scanning of specific target areas, making it suitable for ground vehicles and mapping purposes (Killinger, 2014). LiDAR data were collected using a UAV quadcopter, generating point clouds at a density of 80–85 points/m<sup>2</sup> (Figure 4).

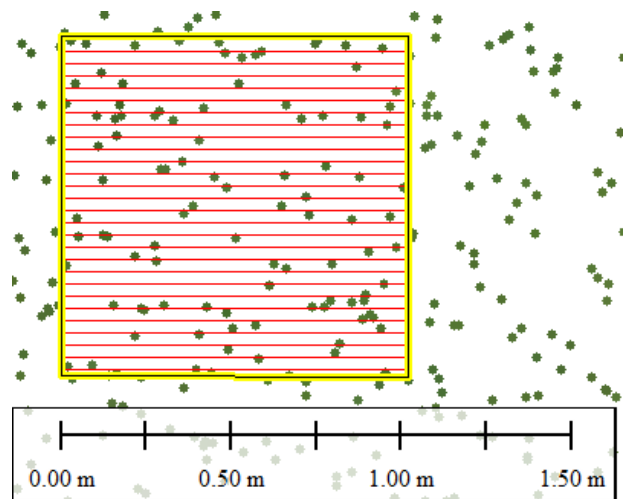


Figure 4 Point cloud density from UAV LiDAR acquisition

Advancements in LiDAR technology support multiple-return detection, which captures more than one reflection from a single laser pulse. This capability is particularly useful for mapping objects with dense canopy, enabling the sensor to differentiate between layered features such as

tree crowns and the ground surface (Ozdemir et al., 2021). Single-return systems record only the first or strongest reflection, capturing vegetation canopy surfaces. Dual, triple, quadruple, and up to penta-return systems record two to five distinct reflections, providing data sets for ground surface extraction (Reutebuch et al., 2003) (Figure. 5). Each return contains spatial and intensity information that varies depending on the material and density of the objects the pulse encounters. This allows estimation of individual tree structures, including crown width, diameter, volume, and height, even when the canopy covers the ground (Maltamo et al., 2004).

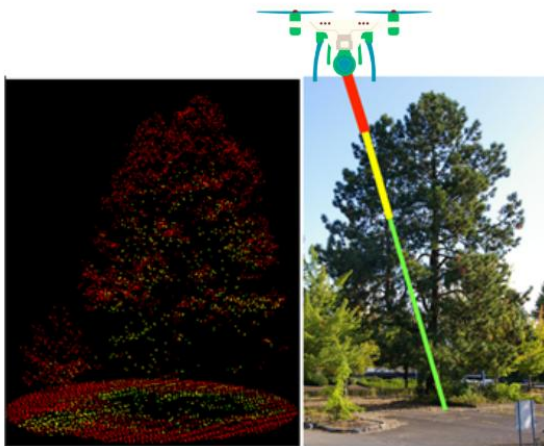


Figure 5 The multiple-return concept: red indicates the first return (leaves), yellow indicates the second return (branches), and green indicates the third return (ground).

#### 2.4. Objects Classification

LiDAR point cloud data classification separates points located on the ground surface from those on objects above the ground. This classification process is crucial for determining the accuracy of topographic mapping. This study employed DJI Terra to classify point clouds into ground and non-ground points using a slope-based approach (Bhattarai et al., 2025). Slope settings were categorized as flat, gentle, and steep to match the field topography. The classification process did not use automated algorithms such as cloth simulation filter or morphological filter; instead, it applied a software-based slope method emphasizing manual parameterization. Consequently, the classification produced ground and non-ground coordinates suitable for accuracy analysis.

#### 2.5. Topographic breaklines

Topographic breaklines are essential features in DEMs because they indicate significant changes in terrain, such as ridges and valleys (Abdullah, 2017). Breaklines play a critical role in hydrological analysis, urban planning, and environmental modeling. Their extraction and application enhance the accuracy of terrain representation, resulting in

more precise topographic analysis (Sakurai et al., 2006). Breaklines are typically derived from field surveys, aerial imagery, or LiDAR data that provide elevation point coordinates. They serve as control boundaries to prevent elevation interpolation from producing surfaces that deviate from actual geomorphology (Febriana, 2018). For example, breaklines along rivers maintain consistent channel edges, preventing water surfaces from appearing elevated relative to banks, while in built-up areas, breaklines preserve object shapes from being truncated during interpolation. This process involves connecting linearly patterned elevation points and integrating them into a Triangulated Irregular Network (TIN) or raster DEM. By doing so, the 3D model can depict ground surface contours more accurately, particularly in areas with steep or complex topography.

#### 2.6. Statistics and Correlation Analysis

This elevation accuracy analysis used two primary datasets: TS acquisition and UAV LiDAR acquisition. TS data served as the reference (ground truth) because it directly measures coordinates in contact with objects. UAV LiDAR data were acquired via aerial surveys, producing three-dimensional point clouds. Processing both datasets yielded elevation values at test points with spatial correspondence.

##### a. Root Mean Square Error (RMSE)

In addition to correlation, the absolute accuracy level was evaluated using the Root Mean Square Error (RMSE), which represents the average magnitude of error between the UAV LiDAR and TS results. The RMSE formula is expressed in Equation (6). (Azmi et al., 2014)

$$RMSE = \sqrt{\frac{1}{n} \sum_{i=1}^n (Z_{LiDAR,i} - Z_{TS,i})^2} \quad (6)$$

Where:

$Z_{LiDAR,i}$ : Elevation value of the  $i$ -th point from UAV LiDAR

$Z_{TS,i}$ : Elevation value of the  $i$ -th point from TS

$n$ : Number of observation points

A smaller RMSE value indicates higher accuracy of UAV LiDAR data relative to the TS reference data.

##### b. Histogram

The distribution of elevation differences ( $Z_{LiDAR} - Z_{TS}$ ) was visualized using an error histogram to illustrate the data spread and bias pattern. The histogram helps identify whether the UAV LiDAR data tend to overestimate or underestimate the reference data and assess the symmetry of the distribution around zero.

##### c. Scatter Plot

The comparative analysis between UAV LiDAR and TS elevations was visualized through a scatter plot to illustrate the degree of agreement between the two datasets. The graph represents the ideal relationship between UAV LiDAR and TS

elevation values, assuming no difference between the two methods, as shown in Equation (7):

$$y = x \quad (7)$$

The actual relationship between the datasets was represented using a linear regression model, as expressed in Equation (8) (Intani, 2019).

$$Y_c = \alpha + \beta_k X_{kc} + \varepsilon_c \quad (8)$$

where:

$Y_c$  = elevation of the c-th point from TS  
 $\alpha$  = constant  
 $\beta_k$  = slope  
 $X_{kc}$  = elevation of the c-th point from LiDAR  
 $\varepsilon_c$  = method-specific error of the c-th point

The slope ( $\beta_k$ ) indicates how closely the LiDAR results correspond to the TS data. The difference between the ideal and regression lines represents the elevation deviation of the UAV LiDAR results.

#### d. Correlation

The correlation analysis measured the strength of the linear relationship between UAV LiDAR elevations (X) and TS elevations (Y). The correlation coefficient (r) was calculated using the Pearson correlation formula (Derber et al., 2015).

$$r = \frac{n\sum XY - (\sum X)(\sum Y)}{\sqrt{[n\sum X^2 - (\sum X)^2][n\sum Y^2 - (\sum Y)^2]}} \quad (9)$$

Where:

$r$ : Correlation coefficient between LiDAR and TS data  
 $X, Y$ : Elevation values from LiDAR and TS  
 $n$ : Number of sample points

The value of  $r$  ranges from -1 to +1. The relationship is categorized as *very strong* if  $r > 0.9$ , *strong* if  $0.7 < r \leq 0.9$ , and *moderate to weak* if  $r \leq 0.7$ . A positive  $r$  indicates a direct relationship between the two elevation datasets.

#### e. Interpretation

The results of the scatter plot, correlation, RMSE, and histogram analyses are complementary. The scatter plot illustrates the relationship pattern between datasets, the correlation quantifies the strength of the linear relationship, the RMSE represents the average vertical deviation, and the histogram reveals the error distribution pattern. Together, these analyses provide a comprehensive assessment of UAV LiDAR elevation accuracy performance under various terrain conditions.

The correlation analysis compared LiDAR elevations against TS measurements using scatter plots of matching test points through coordinate extraction and reference alignment.

$$y = x \quad (6)$$

Indicating no difference between the two methods, while the red line represents the linear regression result, expressed as (Intani, 2019)

$$Y_c = \alpha + \beta_k X_{kc} + \varepsilon_c \quad (7)$$

where:

$Y_c$  = elevation of the c-th point from TS  
 $\alpha$  = constant  
 $\beta_k$  = slope  
 $X_{kc}$  = elevation of the c-th point from LiDAR  
 $\varepsilon_c$  = method-specific error of the c-th point

The slope ( $\beta_k$ ) indicates the closeness of LiDAR results to TS measurements. Deviations between the ideal line and the regression line represent elevation differences of UAV LiDAR measurements.

## 3. Results and Discussion

### 3.1. Analysis of Digital Terrain Model and Contours

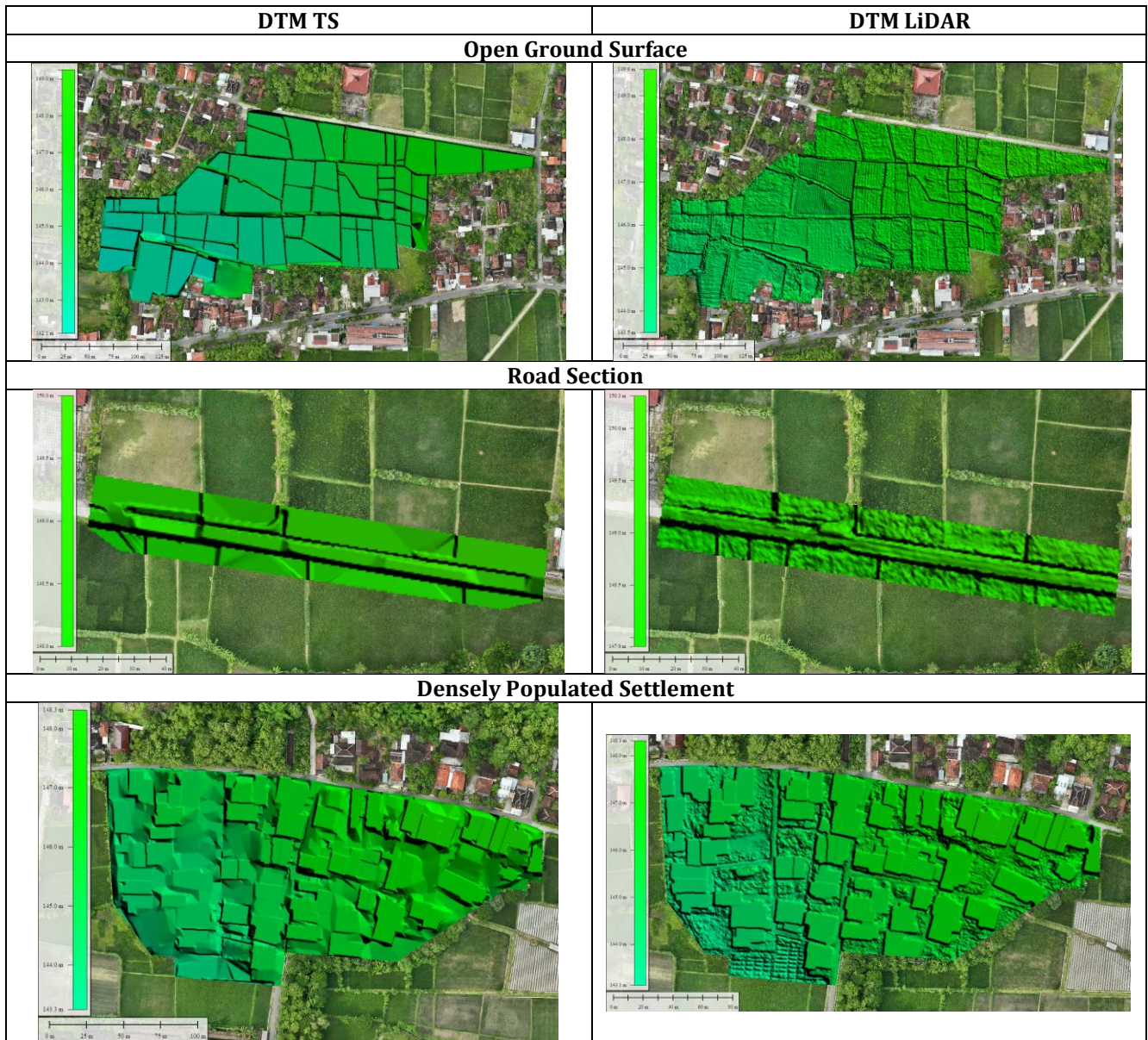
Data acquisition with LiDAR and TS produced 3D coordinates that were analyzed across six area categories: open ground surface, vegetation-covered surface, road section, densely populated settlement, sparsely populated settlement, and river. These 3D coordinates formed the basis for creating the Digital Terrain Model (DTM) (Table 1). Horizontal coordinates (X, Y) represent point positions on the surface, while vertical coordinates (Z) define elevations that form contour lines (Table 2) and their density (Table 3). LiDAR produced a continuous DTM due to its high point density, whereas TS yielded a sparser DTM. In open ground areas, LiDAR produced dense and evenly distributed coordinates, resulting in smooth DTM with clear contours. TS generated fewer points but with high elevation precision, maintaining accurate contours despite lower density. Along road sections, LiDAR provided consistent 3D coordinates representing linear road forms accurately, while TS offered limited but precise coordinates, keeping contours aligned with field conditions. In densely populated settlements, LiDAR often captured reflections from roofs and walls, causing coordinate distortion and unnatural surface contours if ground classification was suboptimal. TS provided precise coordinates in open spaces between buildings, producing more realistic contours despite fewer points. In sparsely populated settlements, LiDAR maintained continuous coordinates with minor distortions, and TS delivered precise coordinates with limited coverage. For rivers, LiDAR struggled to capture the riverbed due to water reflectivity but accurately represented banks, while TS produced highly precise riverbed elevations, forming accurate river contours.

Overall, LiDAR excels in producing 3D coordinates with wide coverage and high density, resulting in continuous

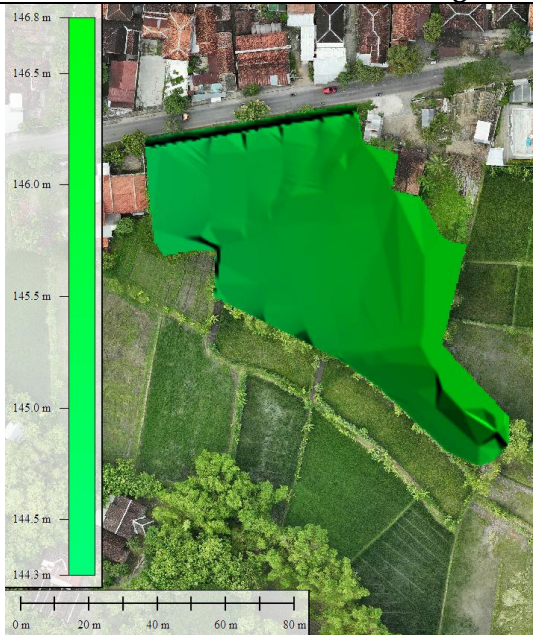
DTM and dense contours. TS excels in coordinate accuracy, particularly in elevation, although point distribution is sparser. To achieve more representative results, LiDAR users should apply filtering, classification, and breakline addition to separate ground from non-ground points and

ensure contours follow actual topography. Combining fast LiDAR acquisition with precise TS measurements provides a balance between data acquisition speed, contour density, and coordinate accuracy.

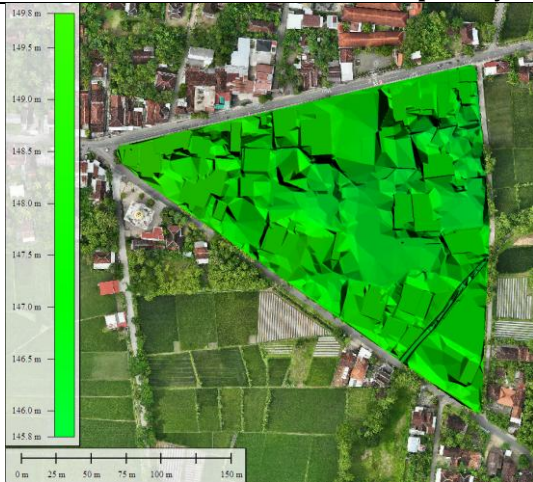
Table 1 DTM Classification by TS and Lidar Method in Different category Areas.



### Vegetation-Covered Surface



### Sparsely Populated Settlement



### River

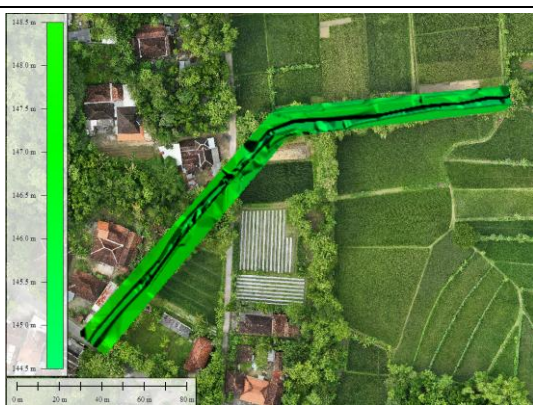
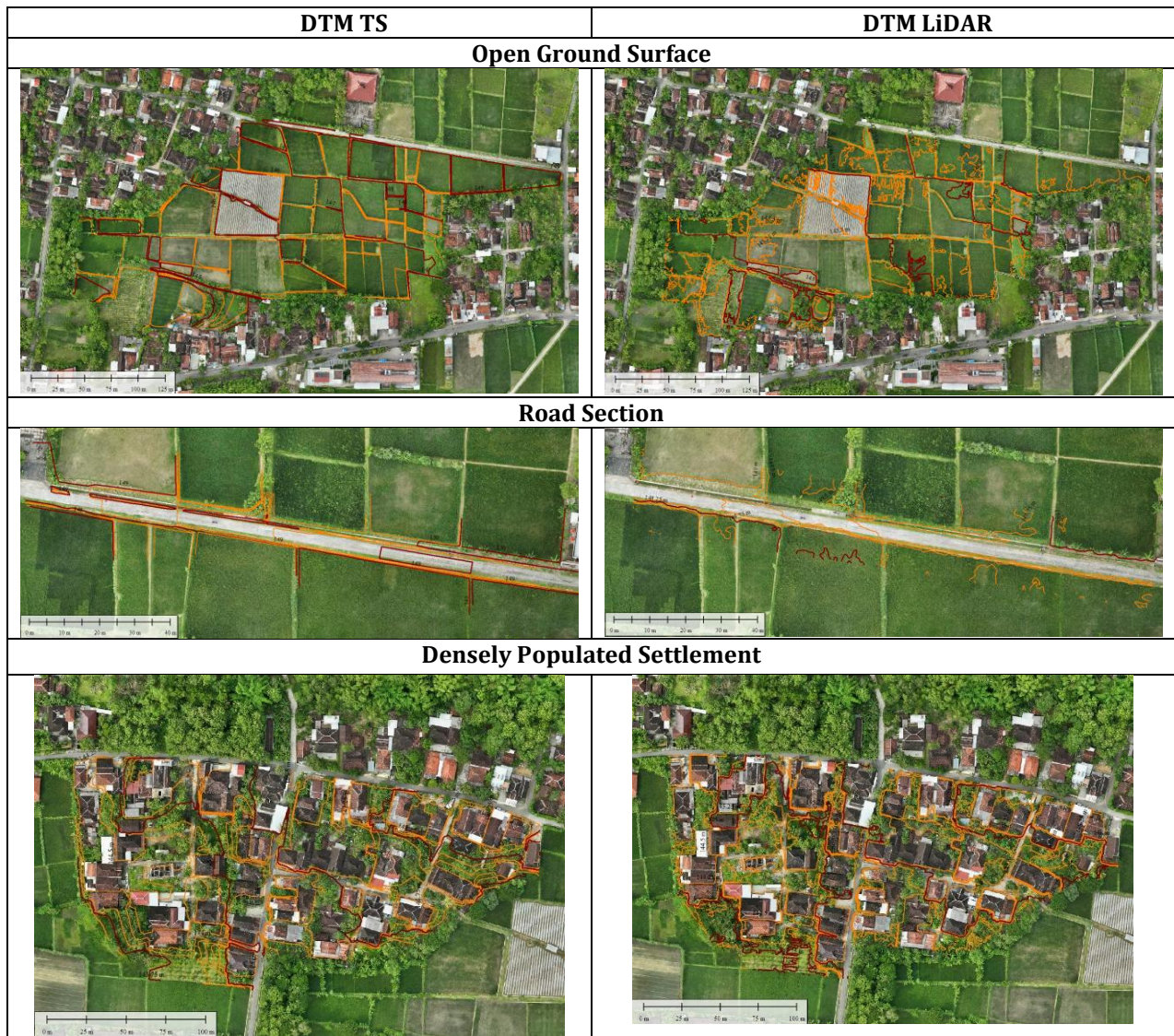


Table 2 Distribution of Major and Minor Contours Generated by TS and Lidar in Different Areas.

Area Category	Major Contours (TS)	Major Contours (LiDAR)	Minor Contours (TS)	Minor Contours (LiDAR)
Open Area	7	6	21	15
Road	2	3	3	6
Vegetation-Covered Area	2	3	7	8
Dense Settlement	5	5	14	14
Sparse Settlement	4	4	11	11
River	4	4	12	10

Table 3. Major (red) and Minor (Orange) Contours by TS and Lidar in Different Areas.





### 3.2. Statistical Analysis of LiDAR Elevations Compared to Total Station

The elevation accuracy analysis employed several statistical approaches, including the evaluation of minimum and maximum elevation values, RMSE, and histogram distribution, to compare LiDAR-derived elevations with TS data. Elevation statistics were analyzed on a 1 m grid for each area to ensure that LiDAR and TS elevations corresponded spatially. The TS data served as the reference because its elevations were measured directly in the field,

while LiDAR data were obtained through aerial acquisition and required validation. The comparison of minimum and maximum elevation values between LiDAR and TS (Table 4) showed that LiDAR results generally aligned with TS measurements across all terrain categories, though slight discrepancies were observed depending on land surface complexity. The smallest differences occurred in sparsely populated settlements and vegetation-covered surfaces, where the minimum elevation deviations were only about 0.24 m and 0.24 m, respectively. In contrast, larger

minimum elevation deviations were found in open ground areas (1.10 m) and road sections (0.09 m). For maximum elevation, LiDAR tended to underestimate TS in open ground surfaces by approximately 2.13 m, while in road sections LiDAR slightly overestimated TS by 0.31 m. When comparing the elevation ranges ( $\Delta_{\max-\min}$ ) between both methods, the differences were generally small, varying from 0.03 m in sparsely populated settlements to 0.22 m in river areas. These variations indicate that LiDAR maintained consistent elevation trends with TS but tended to compress elevation ranges slightly, especially in open and vegetated areas. Such compression reflects LiDAR's tendency to capture slightly lower peaks and higher depressions due to point cloud interpolation and surface smoothing during DTM generation. Overall, these differences demonstrate that LiDAR can reliably reproduce TS elevations under most terrain conditions, though the influence of vegetation, built-up density, and water surfaces can alter the apparent elevation extremes and range.

The histogram analysis (Figure 6) further clarified these variations and complemented the statistical evaluation.

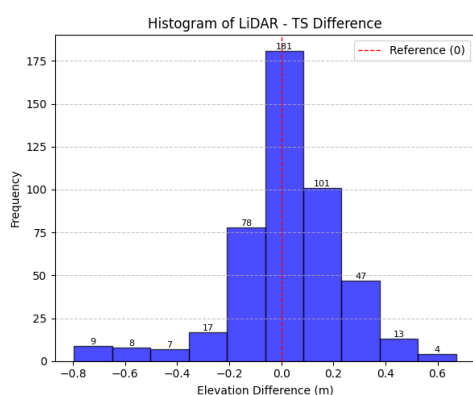
Elevation difference histograms revealed that LiDAR elevations in open ground area and sparsely populated settlements were the most concentrated around zero, indicating a strong agreement with TS data. In contrast, road sections showed a slightly wider spread, reflecting minor irregularities on the road surface and the limited number of samples available in these areas. Vegetation-covered surfaces exhibited positively shifted distributions, suggesting that LiDAR tended to overestimate ground elevations due to canopy returns. Densely populated settlements showed moderately dispersed distributions with positive bias, likely caused by roof and wall reflections. River areas demonstrated the widest and most dispersed patterns, confirming larger elevation deviations associated with LiDAR's reduced capability to penetrate and accurately capture water surfaces. Overall, the histogram analysis reinforced that LiDAR performed best in open and sparsely built environments, while elevation accuracy decreased in areas with dense vegetation, complex structures, or water bodies.

Table 4. Minimum and Maximum Elevation Values of LiDAR and TS DTMs

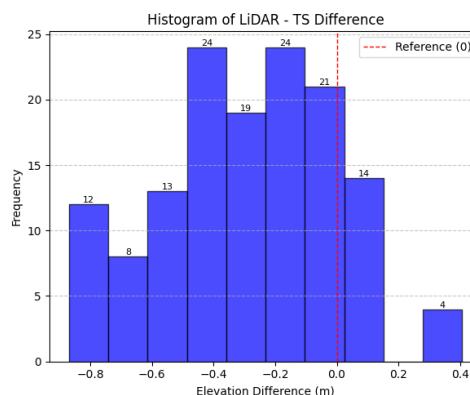
Area Category	Minimum Elev (m)		Maximum Elev (m)	
	Total Station	LiDAR	Total Station	LiDAR
Open Ground Surface,	142.098	140.999	149.250	147.116
Road Section	148.000	147.915	150.000	150.311
Vegetation-Covered Surface	144.250	144.013	146.750	147.245
Densely Populated Settlement	143.250	143.138	148.316	148.316
Sparsely Populated Settlement,	145.750	145.613	149.830	149.833
River	144.500	144.566	148.500	148.731

Quantitative results supported these findings. The smallest RMSE values (Table 5) were observed in road sections (0.031 m) and open ground surfaces (0.046 m), confirming that LiDAR accurately represented flat and unobstructed surfaces. Higher RMSE values were found in vegetation-covered areas (0.164 m), densely populated

settlements (0.107 m), and sparsely populated settlements (0.156 m) due to surface irregularities and land cover interference. The highest RMSE occurred in river areas (0.373 m), emphasizing LiDAR's limitations in capturing accurate elevations over water surfaces.



(a)



(b)

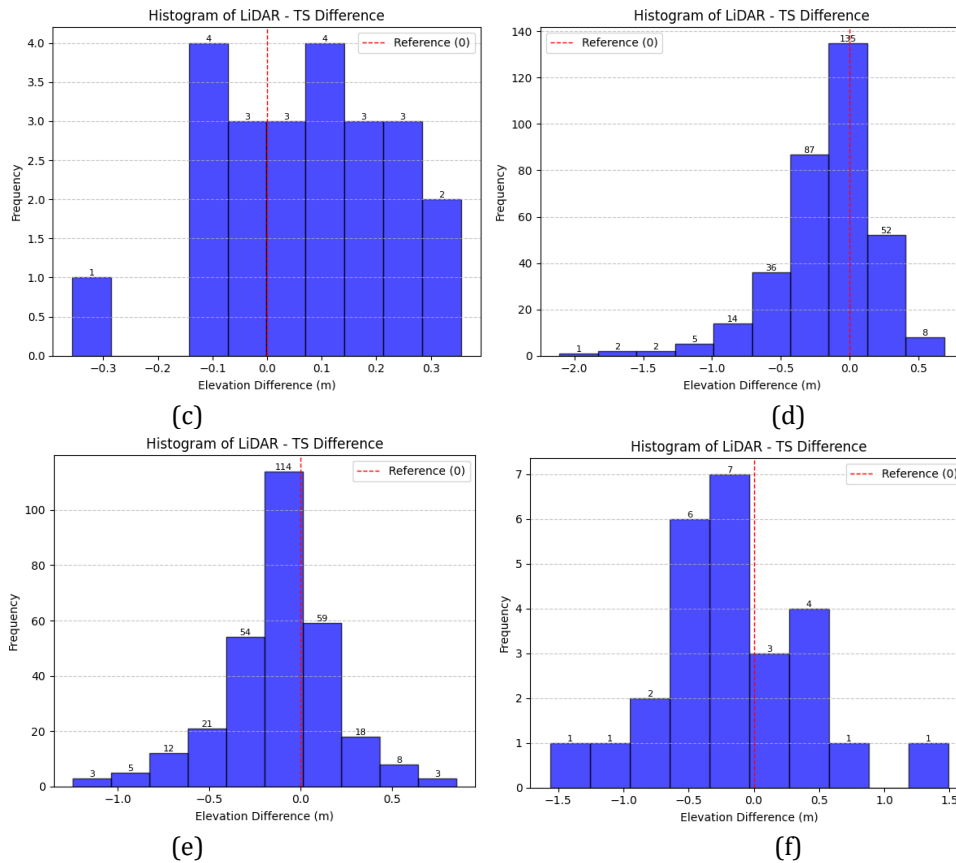


Figure 6. Histogram of elevation differences between LiDAR and TS in (a) open ground surface, (b) vegetation-covered surface, (c) road section, (d) sparsely populated settlement, (e) densely populated settlement, and (f) river.

Table 5 Statistical Summary of Elevation Differences between TS-Derived and LiDAR-Derived DTMs

Area	Elevation Difference (m)		Means (m)	RMSE (m)
	Min	Max		
Open Ground Surface,	0.001	0.796	0.153	0.046
Road Section	0	0.357	0.142	0.032
Vegetation-Covered Surface	0.001	0.869	0.327	0.164
Densely Populated Settlement	0	1.244	0.238	0.107
Sparsely Populated Settlement,	0.002	2.108	0.272	0.156
River	0.059	1.562	0.475	0.373

### 3.3. Correlation of LiDAR Results with TS

The correlation analysis compared LiDAR and TS elevations using scatter plots, with the ideal line  $y = x$  serving as a reference (Figure 7). Elevations point located close to the ideal line indicate strong agreement, between the two datasets, whereas deviations from the line reflect elevation discrepancies. In open ground areas, LiDAR showed a very high correlation with TS, with a regression slope close to 1 and an intercepts of approximately 2.4 m. This indicates that LiDAR elevations slightly overestimated TS elevations but still maintained a consistent linear

relationship. The regression line closely followed the ideal line, confirming that LiDAR accurately represented ground elevations. This finding is consistent with the smallest RMSE value of 0.046 m observed in open ground surfaces.

In road sections, LiDAR also demonstrated strong correlation with TS, though the regression line slightly deviated from the ideal line rather than running parallel to it. This deviation suggests minor systematic bias, likely caused by subtle surface undulations or differences in data alignment. The RMSE of 0.031 m supports this

interpretation, indicating minimal but measurable differences between the two datasets. The generally flat terrain and low obstruction levels in road areas allowed LiDAR to capture ground elevations with high precision.

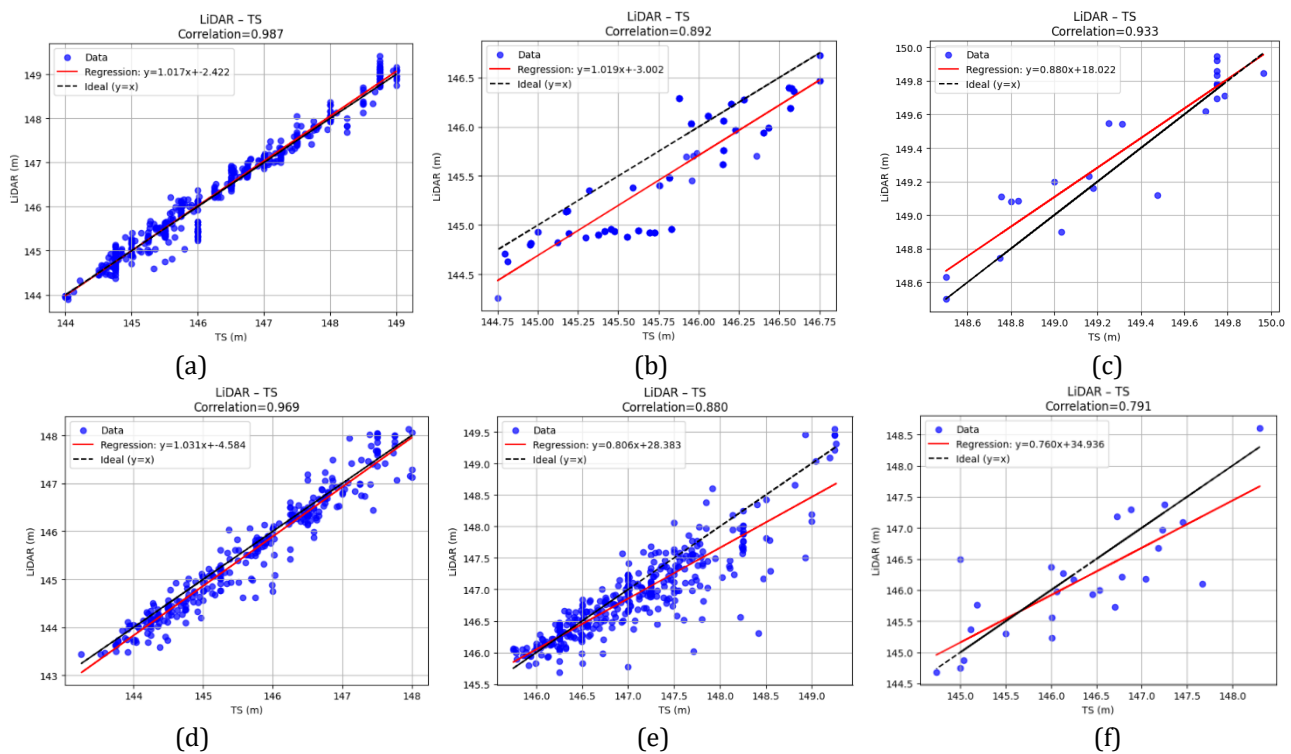


Figure 7. The correlation of elevations between LiDAR and TS was analyzed for the following areas : (a) open ground surface, (b) vegetation-covered surface, (c) road section, (d) sparsely populated settlement, (e) densely populated settlement, and (f) river.

The correlation between LiDAR and TS decreased in vegetation-covered surfaces. Scatter plots showed that the regression line remained relatively close to the ideal line, but the elevation points were more dispersed. Vegetation obstruction caused bias in LiDAR elevations, reflected in an RMSE of 0.164 m. Nevertheless, the correlation remained sufficiently high, indicating that LiDAR could reasonably represent ground elevations after filtering and classification. In densely populated settlements, LiDAR correlation with TS also decreased. The regression line remained near the ideal line, but elevation points showed larger deviations due to reflections from roofs and walls. An RMSE of 0.106 m indicates that LiDAR elevations remained reasonably representative despite deviations in complex areas. Conversely, in sparsely populated settlements, the correlation improved due to reduced obstructions. An RMSE of 0.156 m confirmed that LiDAR elevations in these areas were more consistent compared to densely populated settlements. In rivers, LiDAR correlation with TS dropped significantly due to water surface reflections. Scatter plots showed the regression line still relatively close to the ideal line, but elevation points were widely spread. The highest RMSE of 0.372 m confirmed the largest deviation, indicating that LiDAR was less effective in capturing accurate riverbed

elevations. TS outperformed LiDAR in these conditions by providing precise riverbed measurements.

Overall, the correlation analysis confirmed that LiDAR closely matched TS in flat, open areas, with regression lines almost overlapping the ideal line  $y=x$ . High correlation values accompanied by low RMSE in road and open areas indicate that LiDAR can serve as an alternative for 3D coordinate mapping. However, in dense vegetation, densely built settlements, and water bodies, elevation deviations persisted, requiring LiDAR data to undergo filtering, classification, and breakline processing to achieve elevations closer to actual conditions.

#### 4. Conclusion

Elevation accuracy testing of LiDAR acquisitions against TS across various terrain conditions demonstrated that LiDAR can produce continuous DTMs with high point density, while TS generates sparser but highly precise coordinates. In open ground and road areas, LiDAR elevations closely matched TS results. This was indicated by tightly clustered histograms around zero, very low RMSE values (0.046 m and 0.031 m), and regression lines nearly overlapping the ideal line ( $y=x$ ). These results confirm that

LiDAR is effective for mapping flat, unobstructed areas. In vegetation-covered and settlement areas, LiDAR elevations showed bias due to vegetation obstruction and building reflections. Histograms displayed wider distributions, RMSE values increased (0.106 to 0.164 m), and scatter plot points were more dispersed from the ideal line. Nevertheless, LiDAR still reasonably represented ground elevations after applying filtering, classification, and breakline additions. In river areas, LiDAR elevations exhibited the largest deviations, with an RMSE of 0.372 m due to water surface reflectivity. Scatter plots showed widely dispersed points from the ideal line, reducing LiDAR accuracy. TS remained superior in capturing precise riverbed coordinates because it acquires data directly in the field. Overall, LiDAR is effective for rapid data acquisition in open areas and settlements, whereas TS provides higher precision in complex terrains. Combining both methods offers a balanced approach between acquisition speed and elevation accuracy in accordance with ISO/IEC 17025 standards.

## 5. Funding

This research was funded by Peningkatan Kompetensi Pranata Laboratorium Pendidikan (PKPLP) 2025 from the Directorate of Research Universitas Gadjah Mada.

## 6. Acknowledgment

The authors would like to express their sincere gratitude to the anonymous reviewers for their valuable feedback and constructive suggestions, which significantly improved this study. We are also deeply grateful to the Directorate of Research, Universitas Gadjah Mada, and the Department of Geodetic Engineering, Faculty of Engineering, Universitas Gadjah Mada, for providing the facilities necessary for data acquisition and processing. Most of the figures in this study were generated using QGIS (Nicolas & Frédéric, 2018) and Google Collab.

## 7. Conflict of Interest Statement

The authors declare that we have no conflict of interest related to this study.

## 8. Referensi

- Abdullah, Q. A. (2017). Mapping matters-breaklines for lidar data, do we really need them? In *Photogrammetric Engineering and Remote Sensing* (Vol. 83, Issue 9, pp. 599–602). American Society for Photogrammetry and Remote Sensing. <https://doi.org/10.14358/PERS.83.9.599>
- Azmi, S. M., Ahmad, B., & Ahmad, A. (2014). Accuracy assessment of topographic mapping using UAV image integrated with satellite images. *IOP Conference Series: Earth and Environmental Science*, 18(1). <https://doi.org/10.1088/1755-1315/18/1/012015>
- Basuki, S. (2011). *Ilmu Ukur Tanah* (Cetakan kedua). Gadjah Mada University Press.
- Bhattacharai, A., Scarpin, G. J., Jakhar, A., Porter, W., Hand, L. C., Snider, J. L., & Bastos, L. M. (2025). Optimizing Unmanned Aerial Vehicle LiDAR Data Collection in Cotton Through Flight Settings and Data Processing. *Remote Sensing*, 17(9). <https://doi.org/10.3390/rs17091504>
- Chen, Y., Wang, C., & Li, J. (2015). Hidden target detection from the multi-echo small-footprint LiDAR point clouds. *2015 IEEE 17th International Workshop on Multimedia Signal Processing (MMSP)*, 1–6. <https://doi.org/10.1109/MMSP.2015.7340880>
- Derber, J., Johnson, L., Author, P., Speaker, I., & Radio, F. (2015). *Early Bird Registration Keynote Speakers Matt Simpson the United States Association of Blind Athletes*. [www.afb.org/CVLdirector](http://www.afb.org/CVLdirector).
- Ding, J., & Chen, L. (2024). Application of UAV airborne LiDAR technology in highway engineering construction. *Journal of Physics: Conference Series*, 2863(1). <https://doi.org/10.1088/1742-6596/2863/1/012015>
- Febriana, E. (2018). *ANALISIS METODE HYDRO ENFORCEMENT DALAM PEMBUATAN DIGITAL TERRAIN MODEL LIDAR PADA OBYEK PERAIRAN PETA RUPA BUMI INDONESIA SKALA 1:5000*. Intitut Teknologi Sepuluh November.
- Guth, P. L., Van Niekerk, A., Grohmann, C. H., Muller, J. P., Hawker, L., Florinsky, I. V., Gesch, D., Reuter, H. I., Herrera-Cruz, V., Riazanoff, S., López-Vázquez, C., Carabajal, C. C., Albinet, C., & Strobl, P. (2021). Digital elevation models: Terminology and definitions. *Remote Sensing*, 13(18). <https://doi.org/10.3390/rs13183581>
- Intani, M. M. (2019). *PEMODELAN REGRESI PANEL DENGAN PENDEKATAN MODEL FIXED EFFECT*. UNIVERSITAS BRAWIJAYA.
- Khodabocus, F. (2011). Implementation and Practical Benefits of ISO/IEC 17025:2005 in a Testing Laboratory. In *RESEARCH JOURNAL* (Vol. 17).
- Killinger, D. K. (2014). Lidar (light detection and ranging). *Laser Spectroscopy for Sensing: Fundamentals, Techniques and Applications*, 292–312. <https://doi.org/10.1533/9780857098733.2.292>
- Maltamo, M., Eerikäinen, K., Pitkänen, J., Hyyppä, J., & Vehmas, M. (2004). Estimation of timber volume and stem density based on scanning laser altimetry and expected tree size distribution functions. *Remote Sensing of Environment*, 90(3), 319–330. <https://doi.org/https://doi.org/10.1016/j.rse.2004.01.006>

- Nicolas, M., & Frédéric, P. (2018). Introduction to QGIS. In *QGIS and Generic Tools* (pp. 1–17). John Wiley & Sons, Ltd.  
<https://doi.org/https://doi.org/10.1002/9781119457091.ch1>
- Olawuyi, A. P., & Okeniyi, E. O. (2023). *Accuracy Assessment of Height Difference Using Total Station and Levelling Instrument*. [www.worldscientificnews.com](http://www.worldscientificnews.com)
- Ozdemir, S., Akbulut, Z., Karsli, F., & Acar, H. (2021). Automatic extraction of trees by using multiple return properties of the lidar point cloud. *International Journal of Engineering and Geosciences*, 6(1), 20–26.  
<https://doi.org/10.26833/ijeg.668352>
- Reutebuch, S. E., Mc Gaughey, R. J., Andersen, H. E., & Carson, W. W. (2003). Accuracy of a high-resolution lidar terrain model under a conifer forest canopy. *Canadian Journal of Remote Sensing*, 29(5), 527–535.  
<https://doi.org/10.5589/m03-022>
- Sakurai, Y., Rikimaru, A., & Takahashi, K. (2006). Examination of the SRTM-DEM Subdivision Technique Extracting and Using Topographic Breakline Information. *Journal of The Japan Society of Photogrammetry and Remote Sensing*, 45(5), 46–52.  
<https://doi.org/https://doi.org/10.4287/JSPRS.45.546>
- Saleem, N., Enamul Huq, M., Twumasi, N. Y. D., Javed, A., & Sajjad, A. (2019). Parameters derived from and/or used with digital elevation models (DEMs) for landslide susceptibility mapping and landslide risk assessment: A review. In *ISPRS International Journal of Geo-Information* (Vol. 8, Issue 12). MDPI AG.  
<https://doi.org/10.3390/ijgi8120545>